

Surface irradiation and materials processing using polyatomic cluster ion beams

Gikan H. Takaoka,^{a)} Hiromichi Ryuto, and Mitsuaki Takeuchi

Photonics and Electronics Science and Engineering Center, Kyoto University, Katsura, Kyoto 615-8510, Japan

(Received 10 August 2011; accepted 11 November 2011)

We developed a polyatomic cluster ion beam system for materials processing, and polyatomic clusters of materials such as alcohol and water were produced by an adiabatic expansion phenomenon. In this article, cluster formation is discussed using thermodynamics and fluid dynamics. To investigate the interactions of polyatomic cluster ions with solid surfaces, various kinds of substrates such as Si(100), SiO₂, mica, polymethyl methacrylate, and metals were irradiated by ethanol, methanol, and water cluster ion beams. To be specific, chemical reactions between radicals of polyatomic molecules and surface Si atoms were investigated, and low-irradiation damage as well as high-rate sputtering was carried out on the Si(100) surfaces. Furthermore, materials processing methods including high-rate sputtering, surface modification, and micropatterning were demonstrated with ethanol and water cluster ion beams.

I. INTRODUCTION

Ion-assisted materials processing has generated interest in surface treatments, such as deposition and etching,^{1–4} and has been responsible for advancements of functional materials. Ion beam technology is one example of ion-assisted material processing that has recently attracted attention due to the controllability and variety of ion beams that can be used. For example, the energy, current, and size of the ion beams can be controlled over a wide range by applying electric and magnetic fields, and they are used in applications such as focused ion beams, ion rockets, accelerators, and fusion reactors.^{5–10} In addition, ion beams can transfer mass and material properties, which is not possible with other beams, such as electron or laser beams. By controlling the kinetic energies as well as by selecting the ion species, ion beams can be used for surface treatments such as implantation, sputtering, and deposition.

It is very hard to transfer a high-current beam of low-energy ions, because the space charge effect is enhanced. Highly accelerated ion beams can be used to sputter the material surface; however, they are also responsible for irradiation damage to the surface. There is a trade-off between a high sputtering rate and a low damage irradiation, although material processing with damage-free sputtering is of course desirable. Chemical sputtering results in less irradiation damage than physical sputtering. Because physical sputtering is caused by a transfer of momentum from incident particles to surface

atoms, it results in irradiation damage to the surface of materials. During chemical sputtering, ion bombardment facilitates a chemical reaction that produces weakly bound particles, which are easily desorbed into the gas phase.¹¹ The release of the weakly bound particles is mostly thermally driven, and the irradiation damage caused by ion bombardment is less than that caused by physical sputtering.

In a polyatomic molecule, various kinds of radicals such as alkyl and hydroxyl radicals are available, and these play important roles in chemical erosion and chemical sputtering. For example, hydroxyl radicals are used for surface oxidation and alkyl radicals such as methyl and ethyl radicals are used for chemical sputtering and chemical vapor deposition. In addition, a cluster state of polyatomic molecules has several unique features, for example, the clusters enable a link between the atomic state and bulk state. The physical and chemical properties of clusters are different to those of the bulk state.^{12,13} Using cluster ion beams, simultaneously low-energy and high-current ion beams can be realized. The impact of cluster ions on solid surfaces is characterized by several unique irradiation effects, which include a high energy density, high mass density, multiple collisions, and low-energy-irradiation effects.^{14–18} For example, the high-energy-density irradiation effect enhances the surface temperature of the impact region, which enhances the chemical reactions occurring on the surface. The multiple collision effect enhances the lateral motion of constituent atoms (or molecules) on the surface, which contributes to the formation of a flat surface. Therefore, polyatomic cluster ion beams have unique properties, which allow chemical sputtering and chemical modification of material surfaces

^{a)}Address all correspondence to this author.

e-mail: gtakaoka@kuee.kyoto-u.ac.jp

DOI: 10.1557/jmr.2011.426

to be performed at room temperature by adjusting the incident energy of cluster ions.^{19–22}

Furthermore, the formation of highly functional surfaces can be achieved by surface treatments such as implantation, sputtering, and deposition. The functional properties of materials can be altered by modifying their intrinsic properties using these techniques. In addition, the formation of functional surface structures by sputtering and smoothing at the nanolevel opens up a new field of application for these material processing techniques. With regard to the source materials used for these processes, liquid materials are more appropriate than gaseous materials as they tend to have more radicals in their polyatomic molecules than gaseous materials. In this article, we focus on liquid materials, such as alcohol and water, and produce polyatomic clusters by exploiting an adiabatic expansion phenomenon. Furthermore, the interactions of polyatomic cluster ions with solid surfaces are investigated to clarify the cluster physics and chemistry involved in the materials processing, and the transfer of incident momentum and energy. The surface reaction dynamics are discussed from a theoretical and experimental viewpoint. Applications of the materials processing methods are demonstrated with polyatomic cluster ion beams, including high-rate sputtering of surfaces, surface modification, and micropatterning.

II. EXPERIMENTAL PROCEDURE

A. Cluster ion beam system

Figure 1 is a schematic diagram of the polyatomic cluster ion beam system. The details of the system have been described elsewhere.²³ Liquid materials such as alcohol and water are placed in a metal box, which serves as a source for the production of clusters. The liquid materials are heated up to 150 °C by a wire heater attached around the source, and the vapors of the liquids are ejected through a nozzle into a vacuum region. As shown in Table I, the vapor pressure increases with an increase in the source temperature. The vapor pressure is monitored by a pressure gauge connected to the cluster source. When the vapor pressure is large, for example, 1 atm for ethanol and water or 5 atm for methanol, vaporized clusters are produced by an adiabatic expansion phenomenon without the addition helium gas. The converging–diverging supersonic nozzle is made of glass and has a throat diameter of 0.1 mm.

The produced polyatomic clusters pass through a skimmer and a collimator, and then enter an ionizer. Inside the ionizer, the neutral clusters are ionized by electron bombardment. The electron voltage for ionization (V_e) was adjusted to be between 0 and 300 V, and the electron current for ionization (I_e) was adjusted to be between 0 and 250 mA. The cluster ions are accelerated by applying an extraction voltage to the extraction electrode.

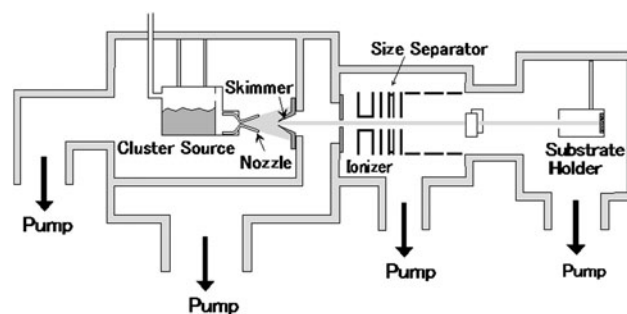


FIG. 1. Schematic diagram of the polyatomic cluster ion beam system.

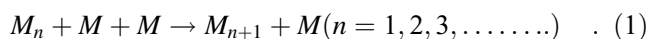
TABLE I. Source temperatures at vapor pressures of 1, 2, 3, and 4 atm for ethanol, methanol, and water.

Liquid	1 atm	2 atm	3 atm	4 atm
Ethanol	351 K	370 K	382 K	391 K
Methanol	338 K	355 K	367 K	376 K
Water	373 K	394 K	407 K	418 K

The extraction voltage was adjusted to be between 0 and 2 kV. The extracted cluster ions are separated according to size using a retardation potential method, and the clusters used were larger than 100 molecules per cluster. The cluster ion beams with large clusters are accelerated toward a substrate, which is placed on a substrate holder. The acceleration voltage (V_a) was adjusted to be between 0 and 10 kV. The beam size at the substrate holder was adjusted by an electrostatic lens to be approximately 2 cm in a diameter. The substrates used were silicon (Si), mica, polymethyl methacrylate (PMMA), and metal films. To allow for a comparison with a Si surface, SiO₂ films were also irradiated by the polyatomic cluster ion beams. The SiO₂ films were thermally grown on the Si substrates to a thickness of 500 nm. A background pressure of 6×10^{-7} Torr was maintained around the substrate using the diffusion pump.

B. Cluster formation

Vaporized-molecule cluster formation can be treated as a gas–fluid phase transition. The theoretical description is based on the three-body collision of a molecule (M), which is described as follows^{24,25}:



If the local temperature is less than the binding energy of the dimer, dimer formation ($n = 2$) is stabilized. After dimers such as M_2 are formed, they act as condensation nuclei for cluster growth. If the ratio of molecules to clusters is high, a cluster growth will occur through the addition of monomers. Thus, nucleation and growth occur through the birth of small molecular clusters that form and grow by molecular collisions. The clusters are

formed in the transition region between hydrodynamic flow and molecular flow. No collision occurs in the molecular flow region.

Classical nucleation theory is based on two fundamental assumptions or approximations, one of which is that classical nucleation is an equilibrium process. Another assumption is that the equilibrium distribution of clusters can be obtained by assuming that the free energy of a cluster is equal to the sum of the free energy of the same number of molecules in the bulk state and the free energy due to the surface of the cluster. The thermodynamic theory shows that the change in the Gibbs free energy (ΔG) during the formation of a cluster of radius r is given by²⁶

$$\Delta G = -\frac{4}{3}\pi r^3 \left(\frac{kT}{V_c}\right) \ln S + 4\pi r^2 \sigma, \quad (2)$$

where V_c is the specific volume per molecule in a cluster, T is the vapor temperature, σ is the surface energy, and S is the saturation ratio (P/P_∞) of the vapor pressure (P) to the equilibrium vapor pressure (P_∞). Table II shows the surface energy of various liquids exposed to the air at room temperature.²⁷ Water has a larger surface energy than alcohols such as methanol and ethanol. It should be noted that the surface energy of a cluster with a radius of r is different from the surface energy of the bulk state. The surface energy of a cluster is given by²⁸

$$\sigma = \frac{\sigma_0}{1 + \frac{2\delta}{r}}, \quad (3)$$

where δ is a correction parameter in the range of 0.25 to 0.6 times the intermolecular distance and σ_0 is the surface energy for a plane surface of the bulk state.

A plot of ΔG versus r , calculated from Eq. (2), has a maximum at a radius of r^* , which is given by

$$r^* = \frac{2\sigma V_c}{kT \ln S}. \quad (4)$$

This is defined as the radius of the critical nucleus. Clusters with a radius smaller than r^* are unstable and dissociate by evaporation. In contrast, larger aggregates

are stable and grow due to the condensation. Taking into account the surface energy, the critical nucleus of water is larger than that of alcohol. Because the critical nucleus is typically of atomic dimensions, the use of bulk thermodynamic quantities for such small clusters is questionable. Instead of the thermodynamic theory, statistical or atomistic theory should be applied to model the nucleus formation and growth.²⁵

Furthermore, the collisions between molecules and clusters increase with increasing vapor pressure, which results in the growth of clusters. According to the thermodynamics and the fluid dynamics, the cluster beam intensity depends on the source pressure (P_0), nozzle diameter (D), and the source temperature (T_0). The cluster beam intensity is also proportional to the scaling parameter (ϕ), which is described as follows^{29–31}:

$$\phi = P_0 D \left(\frac{T_b}{T_0}\right)^q, \quad (5)$$

$$\frac{\gamma}{\gamma - 1} \geq q \geq \frac{1.5\gamma - 1}{\gamma - 1}, \quad (6)$$

where γ and T_b are the specific heat ratio and the boiling temperature of the source materials, respectively. The source temperature is normalized to the boiling temperature. The beam intensity is related to the number of collisions in the vapor during the supersonic expansion and is evaluated by the parameter ϕ . When the nozzle diameter is fixed, the beam intensity increases with increasing source pressure. However, it should be noted that polyatomic clusters consisting of molecules such as water and alcohol contain hydrogen bonds. In this respect, polyatomic clusters are different from monatomic gas clusters such as argon (Ar) clusters, which are loosely coupled to each other by a van der Waals force. Furthermore, because hydrogen-bonded liquids undergo intermolecular interactions such as rotations and vibrations, the theoretical determination of the critical radius and nucleation rate is different than for monatomic clusters. Therefore, a moderate cluster formation and growth is required to generate polyatomic clusters.^{25,32}

C. Size distribution

The cluster size was measured by a time-of-flight (TOF) method. To make a TOF measurement, the accelerated cluster ions first entered a flight tube, and they were deflected by a negative voltage pulse. Due to the application of this voltage, the cluster ions drifted towards a Faraday cup mounted at the end of the flight tube, which detected the ions. The acceleration voltage for the cluster ions was 6 kV, and the pulse voltage was 2 kV. The duration time and the repetition rate of the pulse voltage were 10 μ s and 100 Hz, respectively. The

TABLE II. Surface energy of various liquids exposed to the air at room temperature.

Liquid	Surface Energy σ (dyne/cm)
Methanol	22.6
Ethanol	22.8
Acetone	23.7
Benzene	28.9
Water	72.8
Mercury	435

drift distance was 0.51 m. The cluster size was calculated based on the drift time, which ranged from microseconds to milliseconds and varied depending on the mass of the cluster ions.

Figure 2 shows the size distribution of clusters at different vapor pressures for ethanol clusters, methanol clusters, and water clusters. It was assumed that the cluster ion was a singly charged particle. It was not possible to distinguish between a doubly charged cluster ion and a singly charged cluster ion with half the mass of the doubly charged cluster in the TOF measurement. As shown in Fig. 2, the peak size increases with increasing vapor pressure, and it is approximately 1000 molecules for ethanol clusters, approximately 3000 molecules for

methanol clusters, and approximately 2500 molecules for water clusters at a certain vapor pressure. The values of T_b and γ are 351 K and 1.13 for ethanol and 373 K and 1.33 for water, respectively. In addition, the value of $P_0 (T_b/T_0)^{\gamma/(\gamma-1)}$ at a pressure of 3 atm is 2.1 atm for water and 1.4 atm for ethanol. The size of stable water clusters increases more rapidly with vapor pressure than the size of stable ethanol clusters, and thus, the peak size of water clusters becomes larger than that of ethanol clusters above a certain vapor pressure. As a result, water clusters are easier to produce than the ethanol clusters at the same vapor pressure. With regard to the size of stable methanol clusters, the values of T_b and γ for methanol are 338 K and 1.26, respectively. The value of $P_0 (T_b/T_0)^{\gamma/(\gamma-1)}$ at a pressure of 7 atm is 3.2 atm for methanol, and because of this, methanol clusters can be formed that are larger than the water and ethanol clusters.

III. INTERACTION OF POLYATOMIC CLUSTER IONS WITH SOLID SURFACES

A. Theoretical modeling

A cluster is an aggregate of a few tens to several thousands of atoms (or molecules). The impact effects of cluster ions are quite different to those of monomer ion irradiation. Figure 3 is a schematic illustration of the transfer of incident momentum of cluster ions as well as the physical and chemical sputtering of solid surfaces with polyatomic cluster ions. Because the cluster diameter of several thousand molecules is a few nanometers in size, the clusters penetrate a solid surface over an area of only a few nanometers, which causes multiple collisions between cluster molecules and surface atoms. Therefore, the incident energy of a cluster ion is deposited at the surface of the material, and this dense energy deposition results in an enhancement of the sputtering yield.

In addition to a high sputtering rate, cluster ion irradiation also gives rise to the lateral sputtering effect,^{16,33} which enhances sputtering due to the interaction between the material surface and the shock waves produced by the cluster impact. When cluster ions impact on the solid surface, clusters are broken up into individual molecules, and some molecules also exhibit fragmentation if the incident energy of ions becomes higher. Sputtered particles have a lateral momentum on the surface, and this momentum is expected to cause a smoothing of the surface. As well as the lateral sputtering effect, cluster ions are characterized by low-energy irradiation. Because the kinetic energy of a molecule in a cluster is equal to the total cluster energy divided by the cluster size (i.e., the number of molecules in the cluster), low-energy ion irradiation can be realized using cluster ion beams at relatively high acceleration voltages. Therefore, cluster ion beams cause much less irradiation damage than monomer ion beams.

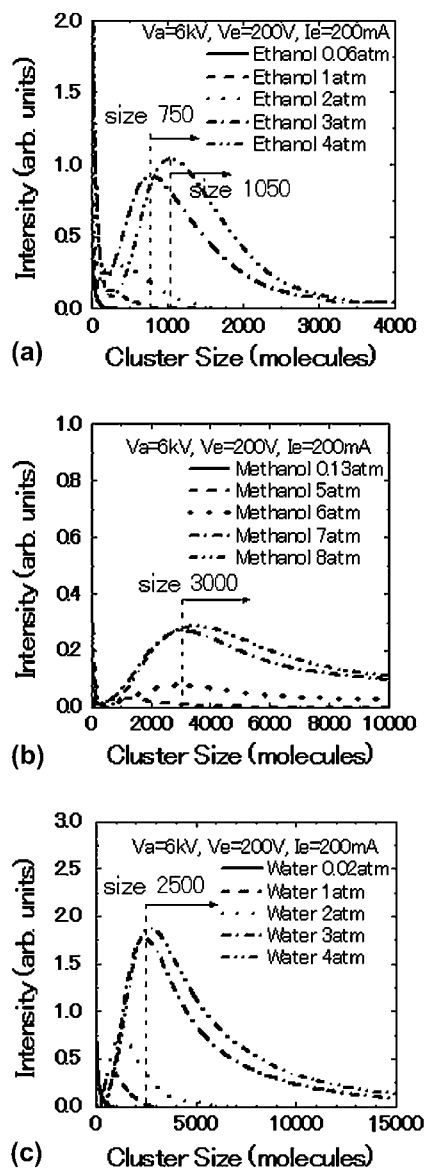


FIG. 2. Size distribution of clusters at different vapor pressures for (a) ethanol clusters, (b) methanol clusters, and (c) water clusters. The acceleration voltage was 6 kV.

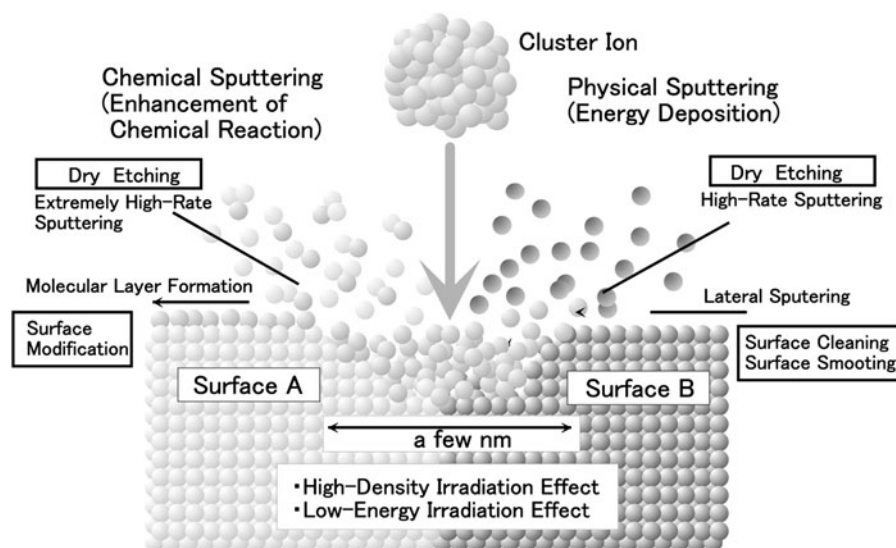


FIG. 3. Schematic illustration of impact of polyatomic cluster ions on solid surfaces.

With regard to the high sputtering rate, chemical and physical sputtering play an important role in cluster ion irradiation even at room temperature. During cluster ion impact, chemical products are produced by the cluster ion irradiation. The rate of chemical reaction (ν) of multiple reaction paths is described as follows³⁴:

$$\nu \propto N \frac{kT}{h} \sum_{i=1}^n \exp\left(-\frac{Q_i}{kT}\right), \quad (7)$$

where N is the number density of polyatomic molecules such as ethanol, methanol, and water molecules, h is Planck constant, k is Boltzmann constant, T is the temperature of polyatomic molecules after impact, Q_i ($i = 1, 2, \dots, n$) is the activation energy for the i th reaction path, and n is the number of each reaction path. The equation indicates that the rate of chemical reaction increases with increasing temperature. Furthermore, the reaction path with the lowest energy barrier will have the fastest reaction rate, and such a chemical reaction will preferentially occur. When polyatomic cluster ions impact on the surface of a solid, the cluster ions are broken up and multiple collisions between polyatomic molecules and surface atoms occur. As a result, many surface atoms are displaced and transferred into a random vibrational state, which results in the local area being in a high-temperature state. Thus, the incident energy of the cluster ions can be used for local heating of the impact region on solid surfaces. In molecular dynamic simulations, the temperature of the cluster impact region was a few tens of thousands of degrees, although the substrate was at room temperature.^{35,36} In this case, the thermal vibration frequency of the polyatomic molecules, which is expressed by kT/h in Eq.(7), would be extremely high. On the other hand, the barrier height for the chemical

reaction is expressed by Q_i/kT , and this becomes relatively low at high temperatures. As a result, several chemical reactions may occur almost at the same time even over a very short time due to cluster ion irradiation, and the enhancement of these chemical reactions is the origin of the high sputtering rate.

During chemical sputtering by ethanol cluster ion irradiation, the dissociation of ethanol molecules is necessary to produce various kinds of radicals. To study the dissociation process of an ethanol molecule, a first-principles calculation was performed using the computer software Materials Studio (Accelrys Co., Tokyo, Japan). Figure 4 shows snapshots of the impact of an ethanol molecule with different incident energies on the Si(111) surface. The bonding energy for the Si–Si bond was assumed to be 2.3 eV. Furthermore, the bonding energy of other bonds such as C–H, C–C, C–O, and O–H in ethanol was fixed at 4.3, 3.6, 3.7, and 4.8 eV, respectively. As shown in Fig. 4, for the incident energy (E_0) of 2.87 eV, the ethanol molecule reflects from the Si surface after impact, and the Si surface deforms without breaking any Si–Si bonds. When the incident energy is 12.0 eV, the ethanol molecules sometimes dissociate on impact into C_2H_5O and H radicals, as shown in Fig. 4(b). The C_2H_5O radical is absorbed into the Si surface, and the H atoms are desorbed from the surface. Si–Si bonds in the surface material are broken, which produces defects. At the incident energy (E_0) of 17.3 eV, more atomic bonds in the ethanol molecules and the Si surface are broken, as shown in Fig. 4(c). These results indicate that there is no irradiation damage at low incident energies, i.e., below a few eV, and the dissociation of the ethanol molecule requires an incident energy of approximately 12 eV. It should be noted from the experimental data that the energy dependence of defect formations on the Si(111) surface

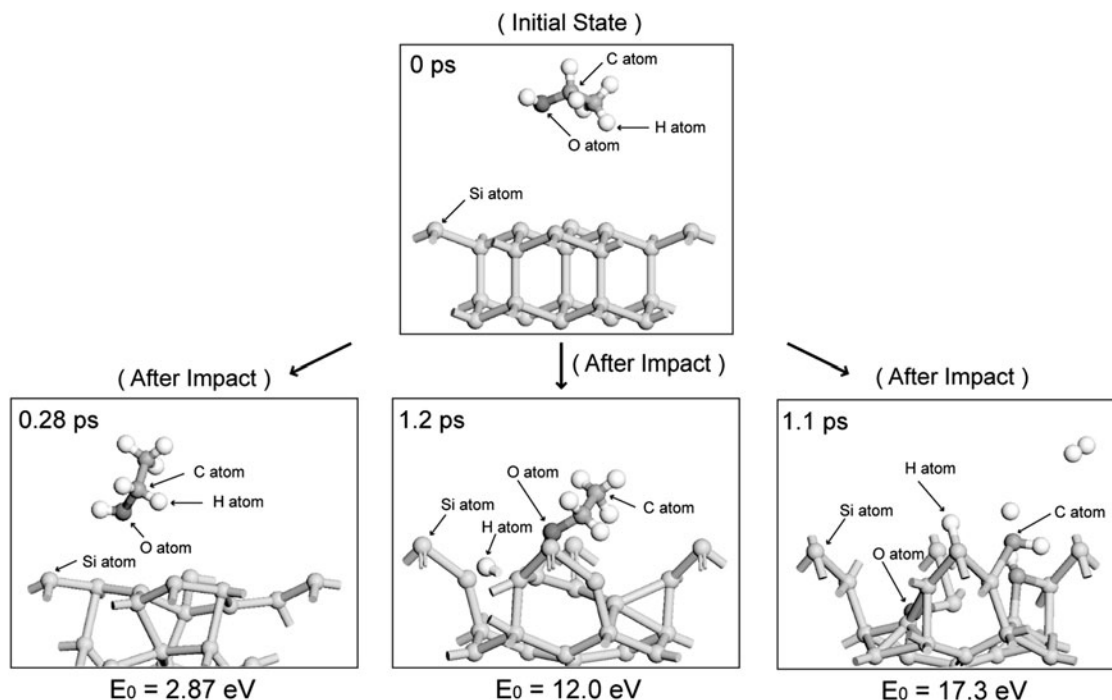


FIG. 4. Snapshots of the impact of an ethanol molecule with different incident energies on the Si(111) surface.

due to cluster ion irradiation was similar to that for the Si (100) surface³⁷ because the Si surfaces were in the amorphous state when irradiated by cluster ions. Therefore, the difference in the surface planes is not sensitive to the surface reaction processes such as absorption and dissociation, which are considered to occur in an energy range of a few electron volts to a few tens of electron volts per molecule under irradiation by ethanol cluster ions.

B. Sputtering rate and chemical reactions

The sputtered depths of Si(100) and SiO₂ surfaces by polyatomic cluster ion irradiation were measured using the DEKTAK-3173933 step profiler by Veeco Instruments (Tokyo, Japan). Figure 5 shows the dependence of sputtered depth on acceleration voltage for alcohol and water cluster ions. The electron voltage for ionization (V_e) was 200 V, and the electron current for ionization (I_e) was 200 mA. The vapor pressure was 3 atm for ethanol and water and 7 atm for methanol. Only clusters larger than 100 molecules per cluster were used, and the ion dose was maintained at 1.0×10^{16} ions/cm². As shown in Fig. 5(a), the Si(100) surfaces are more sputtered than the SiO₂ surfaces, and the sputtered depth increased with increasing acceleration voltage. When the acceleration voltage was 9 kV, the sputtered depth of the Si surfaces by the ethanol and methanol cluster ion irradiation were 475 and 1497 nm, respectively. Taking into account the sputtered depth and the ion dose, the sputtering yield was calculated by first estimating the density of Si and SiO₂ to be 2.42 and 2.63 g/cm³, respectively. The sputtering yield of Si at an

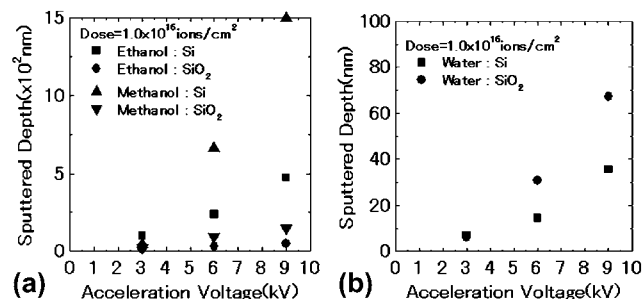
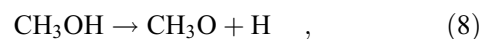
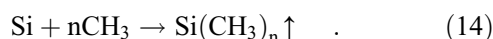
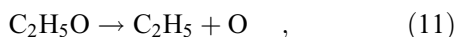
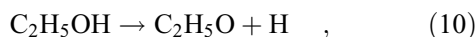


FIG. 5. Dependence of sputtered depth on acceleration voltage for (a) alcohol cluster ions and (b) water cluster ions.

acceleration voltage of 9 kV for the ethanol and methanol cluster ions was found to be 246 and 776 atoms per ion, respectively, which is a few hundred times larger than that obtained using Ar ion beams. The sputtering ratio of Si to SiO₂ is approximately 10. This significant difference in sputtering yields arises from the volatility of the reaction products and the difference in binding energies of the materials. This suggests that the chemical reactions between Si atoms and alcohol molecules produce silicon hydride and silicon hydrocarbon, which are known to be the dominant etching materials for Si surfaces.

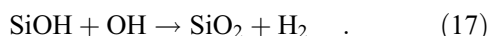
Hydrogen atoms and alkyl radicals play an important role in the chemical sputtering of the Si surfaces. They react with the Si surface atoms as follows:





In these chemical reactions, the silicon hydride and silicon hydrocarbide materials are volatile compounds and are ejected from the substrate surface.

For water cluster ion irradiation, which is shown in Fig. 5(b), the sputtered depths of Si and SiO₂ are very similar. The sputtering yield at an acceleration voltage of 9 kV was 17.8 atoms per ion for Si and 17.1 molecules per ion for SiO₂, which is approximately 10 times larger than that obtained using Ar monomer ion irradiation. After bombardment of the Si surface by the water cluster ions, surface oxidation occurs. The oxidation process of the Si surface is described as follows:



The resulting OH radicals have important roles in the oxidation process due to the implantation and diffusion processes. Because the silicon oxide layer has a higher surface binding energy than the Si surface, there are fewer chemical effects due to sputtering of the oxide layer. Instead, physical sputtering occurs due to the bombardment of cluster ions with a higher energy than a few tens of electron volts per molecule, although the number of cluster ions involved in physical sputtering is small. The incident energy of the cluster ions, which is larger than the chemical sputtering energy, is transferred to the oxide layer by the physical sputtering process. As a result, the sputtered depth of Si surfaces is similar to that of SiO₂ surfaces.

Figure 6 shows the dependence of sputtered depth due to water cluster ion irradiation for Si(100) and SiO₂ surfaces on the ion dose. As shown in Fig. 6, the sputtered depth increases with increasing ion dose. However, the sputtered depth for the Si(100) surface does not increase linearly with increasing ion dose, and it increases gradually toward a certain depth at an ion dose of 1.0×10^{16} ions/cm². At a lower ion dose of

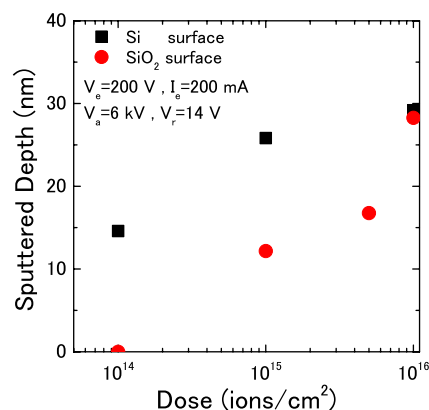


FIG. 6. Dependence of sputtered depth due to water cluster ion irradiation for Si(100) and SiO₂ surfaces on the ion dose.

1.0×10^{14} ions/cm², the ratio of the sputtered depth of the Si(100) surface to that of the SiO₂ surface is approximately 10, which indicates that chemical erosion of the Si surface such as silicon hydride occurs, resulting in an enhancement of the chemical sputtering of the Si surface. When water cluster ions are irradiated on the Si surface, some of the water molecules dissociate into OH radical and hydrogen atom. Therefore, both oxide and hydride reactions on the Si surface occur during the initial stage of irradiation, for example, the formation of silicon oxide and silicon hydride. However, the oxide reaction rather than the hydride reaction increases with increasing ion dose, so that the Si surface becomes oxidized, which results in a decrease in chemical sputtering by the hydride reaction. As a result, the sputtered depth of the Si(100) surface at the ion dose of 1.0×10^{16} ions/cm² is similar to that of SiO₂.

The surface state of the Si(100) substrates after irradiation by the ethanol, methanol, and water cluster ion beams was investigated using x-ray photoelectron spectroscopy (XPS) measurement. Figure 7 shows the depth profile of the XPS peaks for the irradiated Si(100) surface. After etching the surface by 0.5 nm, the oxygen (O1s) and carbon (C1s) peaks in the spectra of samples irradiated by ethanol and methanol clusters disappear, as shown in Figs. 7(a)–7(d). This indicates that ethanol and methanol molecules or their fragments are present on the irradiated Si surfaces, and they are not implanted into the Si surface. On the other hand, the silicon (Si2p) peak for the Si(100) surface irradiated with water cluster ions, which is shown in Figs. 7(e) and 7(f), is shifted to a higher value of binding energy, which corresponds to the peak for SiO₂. The peak decreases with increasing depth, and another peak corresponding to the Si surface is observed. At a depth of 10.5 nm, the SiO₂ peak disappears, and only the Si peak is observed. In addition, the O1s peaks move to a lower value of binding energy at larger depths. The peak intensity decreases with increasing depth, and it is very weak at a depth of 10.5 nm. This indicates that the silicon

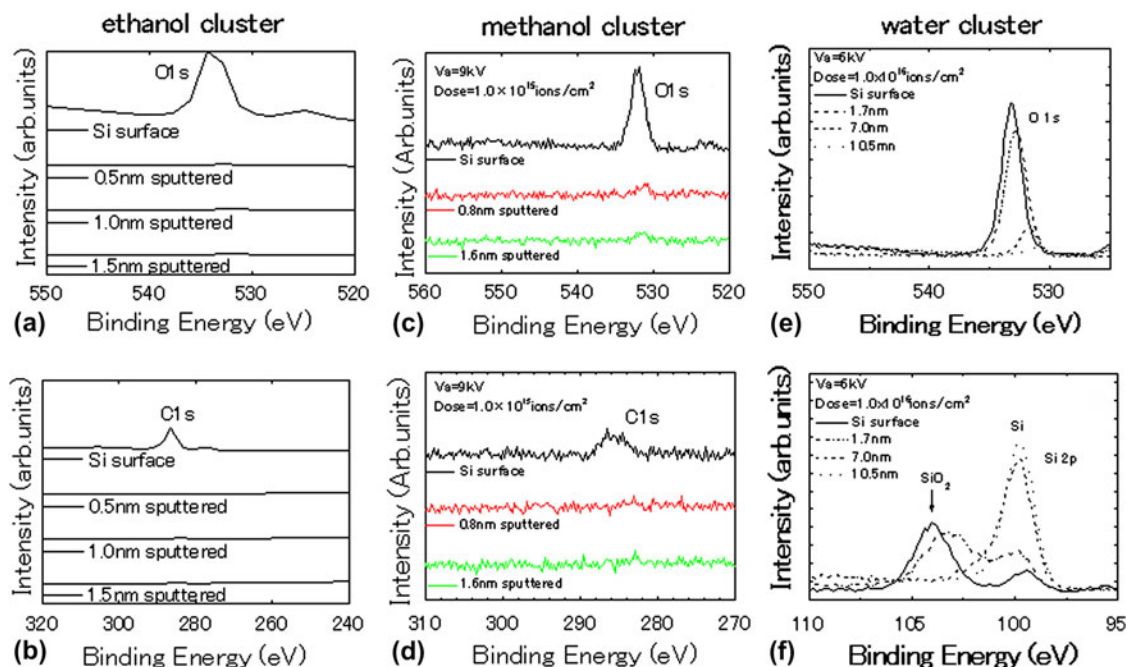


FIG. 7. Depth profile of the x-ray photoelectron spectroscopy peaks for the Si surfaces irradiated by (a, b) ethanol cluster ions, (c, d) methanol cluster ions, and (e, f) water cluster ions.

oxide layer is formed by water cluster ion irradiation, and the oxide layer thickness is approximately 10 nm.

C. Irradiation damage

Low-energy-irradiation effects can be significant for cluster ion beams. The irradiation damage by polyatomic cluster ion beams was investigated using the Rutherford backscattering spectrometry method. Figure 8 shows the number of displaced atoms for the Si(100) surfaces irradiated at different acceleration voltages by alcohol cluster ions and water cluster ions. For comparison, the irradiation damage caused by Ar monomer ion beams is also shown. The electron voltage for ionization (V_e) was 200 V, and the electron current for ionization (I_e) was 200 mA. The ion dose was 1.0×10^{15} ions/cm². The vapor pressure was 3 atm for ethanol and water and 7 atm for methanol. Only clusters larger than 100 molecules per cluster were used. As shown in the figure, the number of displaced atoms increased with increasing acceleration voltage. The number of displaced atoms due to cluster ion irradiation is less than that for Ar monomer ion irradiation at the same acceleration voltage. With regard to cluster ion irradiation, the incident energy of a molecule is the accelerating energy divided by the cluster size, and this is very low. Therefore, irradiation damage caused by alcohol and water cluster ion beams is less than that caused by Ar monomer ion beams. In addition, at an acceleration voltage of 1 kV the number of atoms displaced by ethanol cluster ion irradiation is the same as that of the Si(100) surface prior to irradiation. Because the

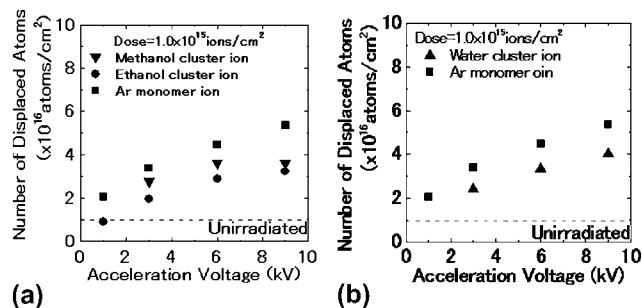


FIG. 8. The number of displaced atoms for the Si(100) surfaces irradiated at different acceleration voltages by (a) alcohol cluster ions and (b) water cluster ions.

incident energy of an ethanol molecule is less than 10 eV, a damage-free surface can be obtained using the low-energy-irradiation effect of the ethanol cluster ion beams.

IV. MATERIALS PROCESSING WITH POLYATOMIC CLUSTER ION BEAMS

A. Exploiting high-rate sputtering

Sputtering has generally been regarded as an undesired effect that destroys the electrodes and the targets in experimental apparatus such as ion sources and electron microscopes. However, in recent years, the sputtering phenomenon has been used in many applications and has become an indispensable technique in deposition, etching, and cleaning processes.^{38–40} A high sputtering rate is a key factor for improving the throughput. The

sputtering yields for various kinds of metal and Si surfaces irradiated by ethanol and water cluster ion beams were investigated.

Figure 9 shows the sputtering yields for Al, Si, Ti, Ni, Cu, Ag, and Au surfaces at an acceleration voltage of 9 kV. Small clusters were separated using the retardation potential method, and the clusters used were larger than 100 molecules per cluster. In Fig. 9, the sputtering yields due to irradiation of Ar monomer ion beams at the same acceleration voltage are also shown, and these agree with the values estimated by computer simulations.⁴¹ As shown in the figure, the sputtering yield due to water cluster ion irradiation is approximately 10 times larger than that caused by Ar monomer ion irradiation. In addition, selective sputtering on different metal surfaces takes place. When this occurs, the water cluster ion irradiation on metal surfaces causes physical sputtering. Even if the incident energy of a water molecule as a constituent molecule of a cluster ion is less than 90 eV per molecule, sputtering can occur. As well as the multiple collision effect, the high-energy-density irradiation effect also enhances the sputtering yield compared with that obtained by Ar monomer ion irradiation.

On the other hand, in the case of ethanol cluster ion irradiation, Al, Ti, and Ni surfaces as well as Si surfaces are sputtered more effectively, and the sputtering yield is approximately 100 times larger than that due to Ar monomer ion irradiation. This is thought to be due to the enhancement of chemical sputtering, in which alkyl compounds of the metal are formed as a volatile product. Alkyl radicals, such as CH_2 , CH_3 , C_2H_4 , and C_2H_5 , are included in an ethanol molecule and are produced after the impact of ethanol cluster ions on the metal surface. These radicals play an important role in the chemical reactions of cluster ions with the atoms on the metal surface. As described previously, based on Eq. (7), all chemical reactions involving these radicals can occur because the impact area of the cluster ions becomes

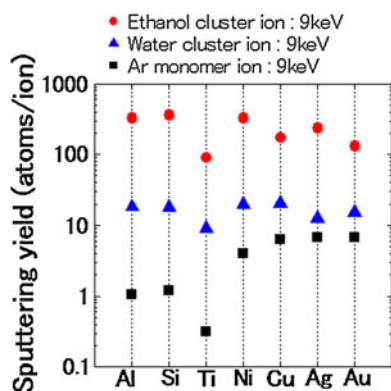


FIG. 9. Sputtering yields for Al, Si, Ti, Ni, Cu, Ag, and Au surfaces by ethanol and water cluster ion irradiation as well as Ar monomer ion irradiation at an acceleration voltage of 9 kV.

extremely hot. Even if the substrate is at room temperature, nonequilibrium chemical reactions take place on the substrate surface in the presence of ethanol cluster ion irradiation. With regard to metal surfaces such as Cu, Ag, and Au, chemical reactions with the alkyl radicals are rare, and the physical sputtering of these metal surfaces occurs due to ethanol cluster ion irradiation.

PMMA is a polymer with a molecular structure of $\text{CH}_3\text{CCH}_2\text{COOCH}_3$. PMMA has attracted interest as an organic glass, and it has been used in various kinds of chemical devices such as microreactors. Figure 10 shows the sputtering yield for PMMA surfaces irradiated at different acceleration voltages by ethanol and water cluster ion beams. Taking into account the sputtered depth and the ion dose, the sputtering yield was calculated by first estimating the density of PMMA to be 1.19 g/cm^3 . As shown in Fig. 10, the sputtering yield increases with increasing acceleration voltage, and the yield was found to be 206 molecules per ion for water cluster ion irradiation and 134 molecules per ion for ethanol cluster ion irradiation at an acceleration voltage of 9 kV. The high sputtering rate of PMMA substrates occurs because of the ejection of sputtered particles as a monomer unit due to the cluster ion irradiation. This is different to the monomer ion irradiation case, where all the bonds in the polymer substrate are easily broken by the irradiation of high-energy monomer ion beams.

Furthermore, water cluster ion irradiation exhibits higher sputtering yields than ethanol cluster ion irradiation at different acceleration voltages, and sputtering even occurs at acceleration voltages lower than 6 kV. For PMMA substrates irradiated by water cluster ions, it is thought that the chemical erosion of the substrate surfaces occurs through the exchange of the CH_3 radical in COOCH_3 with an H atom of the water cluster or through the exchange of an OCH_3 radical with an OH radical. Therefore, the PMMA surface changes to a polymethacrylic acid surface, which has a melting point lower than room temperature and is dissolvable in water. The impact

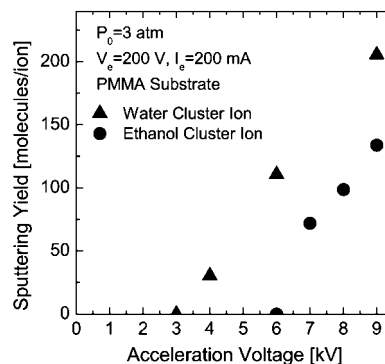


FIG. 10. Sputtering yield for polymethyl methacrylate (PMMA) surfaces irradiated at different acceleration voltages by ethanol and water cluster ion beams.

of water cluster ions on the changed surface enhances the ejection of methacrylic acid molecules in the monomer state from the surface. Thus, the high sputtering rate of PMMA surfaces is achieved by both the chemical erosion of the surface and the momentum transfer of the incident energy of the water cluster ion irradiation.

B. Tailoring the surface morphology

The cluster ion beam process results in unique surface morphology characteristics after bombardment compared with conventional monomer ion beams. When a cluster impacts on a solid surface, a crater structure is formed due to multiple collisions as well as the energy transfer of the cluster ion to the surface.⁴² The single trace of a cluster impact has been studied with atomic force microscopy (AFM), and the crater diameter was measured from an AFM image. Figure 11 shows the AFM image of the mica substrate surface prior to irradiation and a single crater image of a 9 keV ethanol cluster impact on the substrate surface. The irradiation with ethanol cluster ions was performed at an ion dose of 1.0×10^{10} ions/cm² to prevent overlapping of the craters. An AFM image of the mica surface at the atomic level is shown in Fig. 11, although the depth resolution of the AFM is affected by the shape of the tip. The mica substrate is a good choice for the AFM observation to trace the impact of a single cluster ion. In addition, a donut shaped trace is observed on the mica surface irradiated by the ethanol cluster ions, and the inside and outside diameters of the crater are approximately 7 and 17 nm, respectively. This diameter is larger than that of the few nanometer diameter of a single cluster, and an increase in this diameter occurs due to an enhancement of the dissociation of ethanol molecules after impacts of high-energy cluster ions. Thus, the crater is formed due to the high density and nonlinear irradiation effects of ethanol cluster ions irradiation, although crater formation is not realized through a linear cascade of binary collisions caused by impacts of monomer ions.

Figure 12 shows AFM images for the mica surfaces irradiated by ethanol cluster ions at acceleration voltages of 3, 6, and 9 kV. The ion dose was 1.0×10^{12} ions/cm², and the clusters used were larger than 100 molecules per cluster. As shown in Fig. 12, the number and the average diameter of the impact trace increase with increasing acceleration voltage. A few traces were observed with an acceleration voltage of 3 kV, and the number of traces was approximately 0.01 times smaller than the ion dose. This indicates that the threshold energy for formation of a trace on the mica substrate is approximately 30 eV per molecule because cluster ions smaller than 100 molecules were removed from the beam. When the acceleration voltage is larger than 3 kV, the number of traces increases with increasing acceleration voltage. This is ascribed to the fact that the number of cluster ions with incident energy larger than the threshold energy increases with increasing acceleration voltage.

Physical sputtering by cluster ion irradiation is an effective technique to reduce the surface roughness. However, when the initial surface is smooth, i.e., with a roughness less than 1 nm, the irradiated surface becomes rough. This is ascribed to the irradiation effect of cluster ions with a diameter of a few nanometers. Furthermore, for the case of chemical sputtering by cluster ion irradiation, the surface roughness increases with an increase of the sputtered depth. This is similar to other chemical etching processes such as plasma and conventional ion beam methods. Therefore, the surface roughness changes depend on the irradiation conditions such as the incident energy and ion dose.

The sputtered Si surfaces were measured by using the AFM. Figure 13 shows the surface morphology for the Si(100) substrates sputtered by ethanol, methanol, and water cluster ion beams. The acceleration voltage was 6 kV, and the ion dose was 1.0×10^{16} ions/cm². An AFM image of the substrate prior to irradiation is also shown in the figure, and the surface roughness was 0.18 nm.

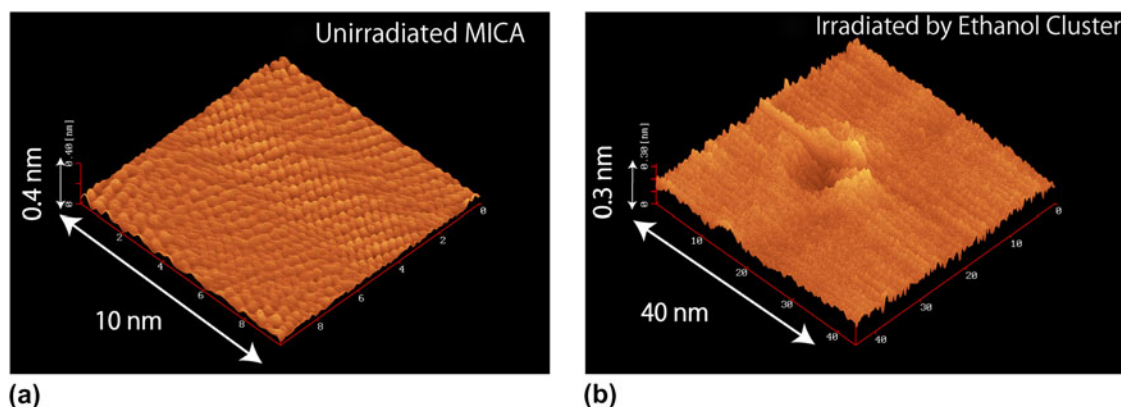


FIG. 11. (a) Atomic force microscopy (AFM) image of the mica substrate surface prior to irradiation and (b) a single crater image of a 9 keV ethanol cluster impact on the substrate surface.

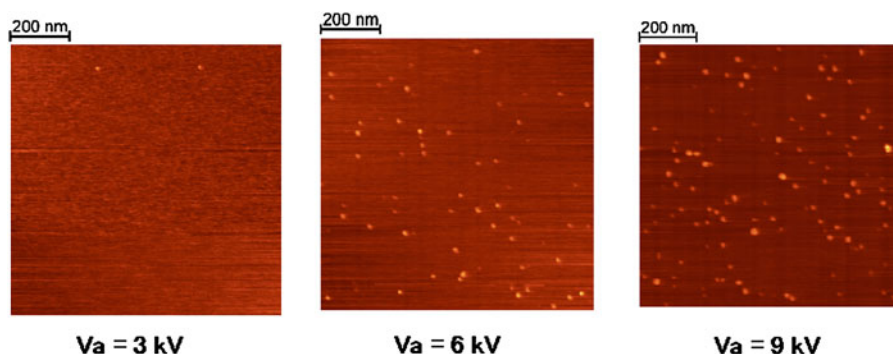


FIG. 12. AFM images for the mica surfaces irradiated by ethanol cluster ions at an acceleration voltage of (a) 3, (b) 6, and (c) 9 kV.

Compared with Si(100) surface prior to irradiation, the sputtered Si(100) surfaces become rough and the surface roughness was 0.93 nm for ethanol cluster ion irradiation, 2.08 nm for methanol cluster ion irradiation, and 0.78 nm for water cluster ion irradiation. Although polyatomic cluster ion irradiation exhibits a high sputtering rate, it results in a smooth surface at the nanolevel even after sputtering.

C. Change in surface wettability

Surface modification is an advanced method for tailoring material properties, which has a central role in chemical, biological, and materials science, and in applied science and engineering.^{43–45} The modification of the hydrophilic and hydrophobic properties of material surfaces is very important, and the control of these properties has attracted much attention. Furthermore, the wettability of surfaces is influenced by the presence of polar groups and the surface roughness. The wettability of substrate surfaces irradiated by ethanol and water cluster ion beams was investigated by measuring the contact angles for water droplets, which were placed on the surfaces immediately after removable from a vacuum chamber. Figure 14 shows the contact angles for Si(100) surfaces irradiated at different acceleration voltages by ethanol and water cluster ion beams. The ion dose was 1.0×10^{15} ions/cm². Cluster larger than 100 molecules per cluster was used. In Fig. 14, the contact angle for the surface prior to irradiation is also shown. As shown in Fig. 14, the contact angle increases with increasing acceleration voltage of ethanol cluster ions, and the hydrophobic property of the Si(100) surface is enhanced at higher acceleration voltages. The contact angle for the Si(100) surfaces irradiated by the ethanol cluster ions may decrease with increasing acceleration voltage because the surface roughness increases with increasing acceleration voltage. However, our results exhibit the opposite behavior, and this is not due to the topological change of the Si(100) surface. This is ascribed to the chemical adsorption of ethanol molecules on the Si(100) surface.

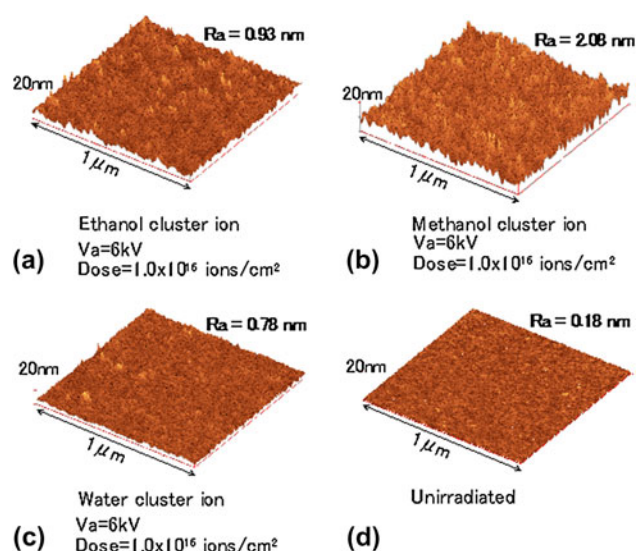


FIG. 13. Surface morphology for the Si(100) substrates sputtered by (a) ethanol, (b) methanol, and (c) water cluster ion beams. The acceleration voltage was 6 kV and the ion dose was 1.0×10^{16} ions/cm².

For ethanol cluster ion irradiation, dissociative adsorption of an ethanol molecule occurs and surface bonds such as hydrogen and ethoxy (C_2H_5O) groups form through the scission of O–H bonds.^{46–48} In the adsorption reactions, the ethoxy groups are oriented such that the axis of the methyl group is nearly perpendicular to the surface, unlike the case for ethoxy groups bound to metal surfaces. Because the methyl group is hydrophobic, the number of these groups increases with increasing acceleration voltage, resulting in an increase in the contact angle.

In contrast, for the case of water cluster ion irradiation, the contact angle decreases with increasing acceleration voltage, and the hydrophilic property of the Si(100) surface is enhanced at higher acceleration voltages. As a result, the wettability of the Si(100) surface is greatly enhanced by the irradiation of the water cluster ions. This is ascribed to the chemical modification of the Si(100) surfaces by the OH radicals, which are produced after

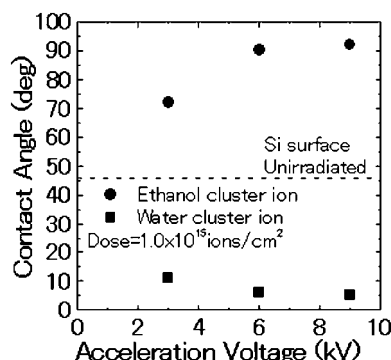


FIG. 14. Dependence of contact angles for Si(100) surfaces irradiated by ethanol and water cluster ion beams on the acceleration voltage. The ion dose was 1×10^{15} ions/cm².

cluster ions impact the Si(100) surfaces. Therefore, the dangling bonds produced on the Si(100) surfaces are bound to the ethoxy groups through an oxygen atom for ethanol cluster ion irradiation and to the hydroxyl radicals for the water cluster ion irradiation. Because of this, a large range in surface wettabilities is accessible by adjusting the acceleration voltage of the ethanol and water cluster ions.

To clarify the difference between the chemical modification of the Si(100) surfaces caused by ethanol and water cluster ion irradiation, the optical transmittance was measured by Fourier transformed infrared spectroscopy (FTIR). Figure 15 shows the transmittance of the Si(100) surfaces irradiated by ethanol and water cluster ions for the wave numbers of 2700–3200 cm⁻¹ and 800–1300 cm⁻¹, respectively. For the ethanol cluster ion irradiation, vibration peaks around 3000 cm⁻¹ appear in the FTIR spectra. These peaks correspond to CH₃ and CH₂, which are not observed in the spectra for water cluster ion irradiation. On the other hand, in the spectra between 800 and 1300 cm⁻¹, vibration peaks representing molecules such as Si–O–Si, Si–OH, and SiH₃ appear for water cluster ion irradiation. These peaks are not observed in the spectra for the ethanol cluster ion irradiation. Taking into account the contact angle measurement for the irradiated surfaces, the Si(100) surface atoms form a bond with the alkyl radicals after ethanol cluster ion irradiation and with the hydroxyl radicals after water cluster ion irradiation.

The wettability of the titanium (Ti) surfaces irradiated by ethanol and water cluster ion beams was investigated. Figure 16 shows the dependence of the contact angles on the acceleration voltage used for the cluster ion irradiation. The ion dose was 1.0×10^{15} ions/cm². The clusters used were larger than 100 molecules per cluster. The contact angle for the surfaces prior to irradiation was also measured, and it was approximately 30°. As shown in Fig. 16, the contact angle for ethanol cluster ion irradiation decreases with increasing acceleration voltage, and it is less than 10° at an acceleration voltage larger than 6 kV.

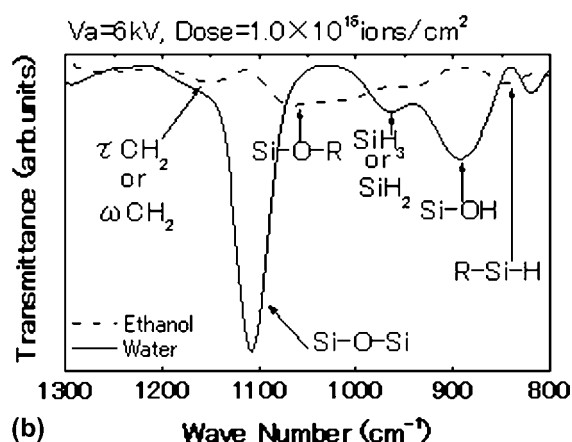
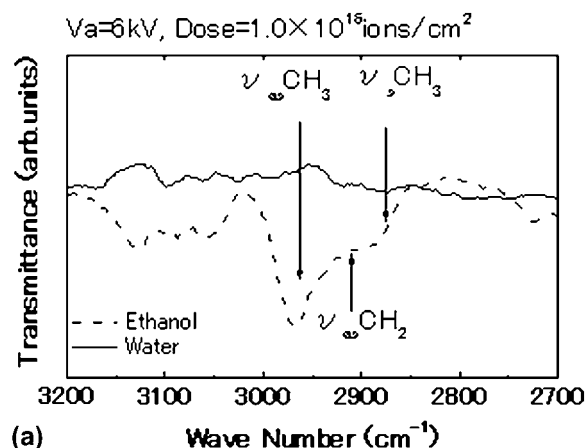


FIG. 15. Transmittance of the Si(100) surfaces irradiated by ethanol and water cluster ions for the wave numbers of (a) 2700–3200 cm⁻¹ and (b) 800–1300 cm⁻¹, respectively.

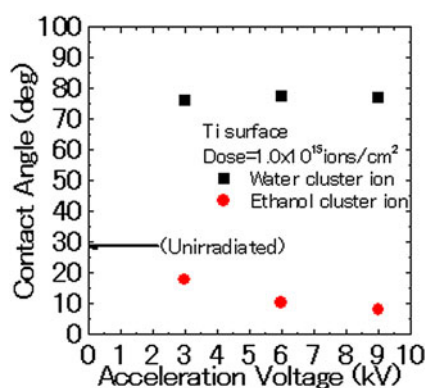


FIG. 16. Dependence of the contact angles for Ti surfaces irradiated by ethanol and water cluster ion beams on the acceleration voltage. The ion dose was 1×10^{15} ions/cm².

From quadrupole mass spectroscopy measurement, it was found that fragmentation of the ethanol molecules occurred after impact of ethanol cluster ions, in which the main fragment was a CH₂OH radical. Therefore, the CH₂OH radical is connected to the Ti surface atoms through Ti–CH₂ bonding, and the top radical of this bond,

i.e., an OH radical, enhances the wettability of the Ti surface. On the other hand, the contact angle for water cluster ion irradiation becomes large at various acceleration voltages, and it is approximately 80° . The Ti surface becomes hydrophobic as a result of water cluster ion irradiation. This is ascribed to the chemical modification of the Ti surfaces by the OH radicals, which are produced after the water cluster ions have impacted on the surfaces. The dangling bonds produced on the Ti surfaces share a bond with the OH radicals, which results in the formation of a titanium oxide layer on the surfaces. Thus, surface modification for Ti surfaces is performed through the attachment of radicals, and it varies depending on cluster ion species as well as the irradiation conditions e.g., the acceleration voltage. In addition, surface modification by polyatomic cluster ion beam irradiation is similar to the formation of self-assembled monolayers, e.g., gold and thiol, which occur during a wet process.^{49–51} This is expected to open up new fields in materials processing.

D. Micropatterning

To demonstrate an engineering application of high-rate sputtering and low-damage irradiation by ethanol cluster ion beams, a patterning process was performed on the Si(100) surface with a photo resist mask. Line, circle, and square mask patterns were commercially available and were prepared on a Si(100) substrate by Yamanaka Semiconductor Co. Ltd (Kyoto, Japan). The line width was in the range of 0.5 to 3 μm . The thickness of the photo resist film coated on the Si(100) substrate was approximately 1 μm . Figure 17 shows the scanning electron microscope (SEM) images for the lines patterned with ethanol cluster ion beams. The acceleration voltage was 9 kV, and the ion dose was 5.0×10^{15} ions/cm². After the ethanol cluster ion irradiation, the photo resist film on the Si(100) surface was removed by rinsing with acetone. As shown in the figure, the edge with a line width of 3, 1, and 0.5 μm is straight, and the micropattern has been clearly prepared by the ethanol cluster ion beam. Also, the measured sputtered depth was approximately 0.22 μm , and this increased with the increase of the ion dose. A sputtered depth of 0.75 μm was obtained at the ion dose of 2×10^{16} ions/cm², and the maximum depth available was limited by the resist film thickness.

Figure 18 shows SEM images for plane views of circle and square patterns with convex pattern and concave patterns prepared on the Si(100) surfaces by irradiation of ethanol cluster ions. The acceleration voltage was 9 kV, and the ion dose was approximately 5.0×10^{15} ions/cm². The diameter of the circle and the edge length of the square were both 60 μm , and the spacing for the circle and square patterns was 10 μm . As shown in Fig. 18, the pattern edge is sharp and the sputtered surface (bright area) is a flat plane. The convex and concave patterns are both similar

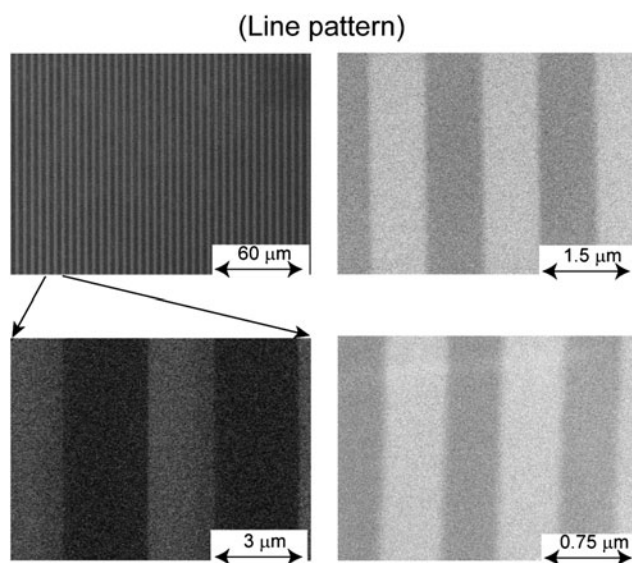


FIG. 17. Lines patterned at a microscale with the ethanol cluster ion beams. The acceleration voltage was 9 kV, and the ion dose was 5.0×10^{15} ions/cm².

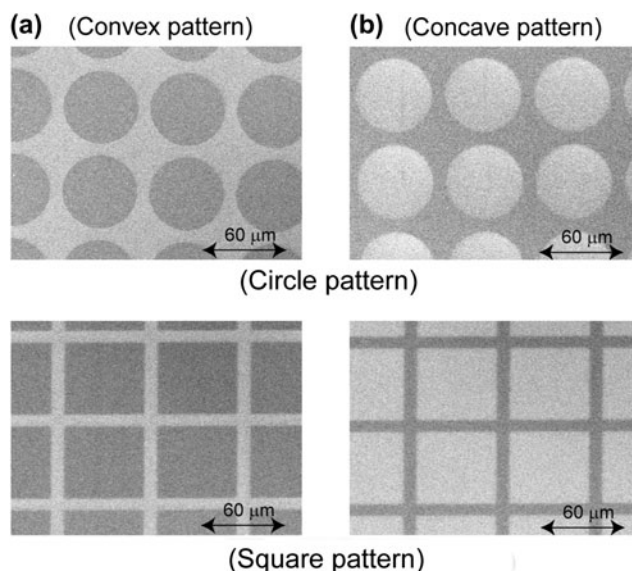


FIG. 18. Scanning electron microscope images for plane views of circle and square patterns with (a) convex pattern and (b) concave pattern prepared on the Si(100) surfaces by irradiation of ethanol cluster ions. The acceleration voltage was 9 kV, and the ion dose was approximately 5.0×10^{15} ions/cm².

to the mask patterns, and the detailed periodic structures such as circles and squares could be prepared using ethanol cluster ion irradiation. This is ascribed to the chemical sputtering of the Si(100) surface by the directional ethanol cluster ion beams, which occurs preferentially over physical sputtering. Most of the volatile particles ejected from the Si surface may evaporate in normal direction, even after they migrate towards the corner or the edge of the pattern.

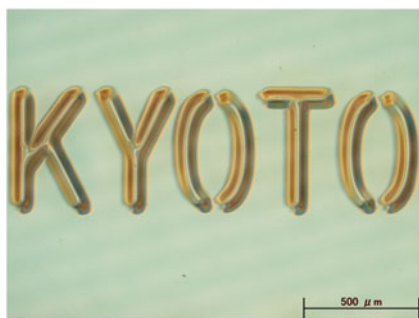


FIG. 19. Micropatterning of a PMMA substrate demonstrated with water cluster ion beams. The acceleration voltage was 9 kV, and the ion dose was 3.0×10^{16} ions/cm².

Figure 19 shows the micropatterning of a PMMA substrate demonstrated with water cluster ion beams. The acceleration voltage was 9 kV, and the ion dose was 3.0×10^{16} ions/cm². As shown in the figure, a micropattern representing the letters “KYOTO” was etched onto the PMMA substrate and the sputtered depth of the substrate was approximately 10 μm. The high sputtering rate of the PMMA substrate is due to the chemical sputtering by water cluster ion irradiation. However, the width of a letter prepared by water cluster ion irradiation is larger than the original one, i.e., >50 μm. This increase of the width is ascribed to the surface diffusion of water molecules on the PMMA surface under the mask by the water cluster ion irradiation. If the contact of the mask on the substrate could be improved, a sharp-edged pattern would be achieved.

V. CONCLUSIONS

We developed a polyatomic cluster ion beam system for materials processing, and various kinds of clusters such as ethanol, methanol, and water clusters were produced by using the adiabatic expansion phenomenon. The intensity of the clusters increased with increasing vapor pressure, and the peak size was approximately 1000 molecules per cluster for ethanol clusters, approximately 3000 molecules per cluster for methanol clusters, and approximately 2500 molecules per cluster for water clusters. The cluster formation of pure vapors was discussed, and the surface energy as well as the specific heat ratio and the boiling temperature were found to influence the cluster formation.

To investigate the interactions of polyatomic cluster ions with solid surfaces, Si(100) substrates and SiO₂ films were irradiated at different acceleration voltages. The ratio of sputtered depth for Si(100) and SiO₂ surfaces was approximately 10 for ethanol and methanol cluster ion irradiation, and the sputtering yield of Si(100) surfaces at an acceleration voltage of 9 kV was a few hundred times larger than that obtained by Ar monomer ion irradiation. The chemical sputtering of Si surfaces by ethanol and methanol cluster ion beams was enhanced through the

transfer of incident energy even at room temperature. Based on theoretical modeling, highly dense energy deposition enhanced the temperature of the cluster impact region, and several chemical reactions leading to chemical sputtering occurred almost at the same time even over a very short time. On the other hand, for the water cluster ion irradiation, the ratio of the sputtered depth for Si(100) and SiO₂ surfaces was almost unity at an ion dose of 1.0×10^{16} ions/cm², and the physical sputtering of Si(100) surfaces was found to occur through surface oxidation. However, at a lower ion dose of 1.0×10^{14} ions/cm², the chemical sputtering of the Si(100) surface through silicon hydride occurred, and the sputtering yield was larger than that of an SiO₂ surface. Furthermore, with regard to the irradiation damage of Si(100) surfaces, the number of atoms displaced by ethanol, methanol, and water cluster ion irradiation was smaller than that displaced by Ar monomer ion irradiation. Also, the surface roughness of Si(100) surfaces increased after sputtering, and it was still less than a few nanometers. Thus, polyatomic cluster ion beams demonstrate unique irradiation effects, which have not been obtained by conventional monomer ion beams.

With regard to materials processing using ethanol and water cluster ion beams, various kinds of substrates such as Si(100), mica, PMMA, and metals were irradiated at room temperature by adjusting the acceleration voltage. The polyatomic cluster ion beams exhibited a high sputtering rate and selective sputtering for these substrates. To demonstrate an engineering application of high-rate sputtering as well as low-irradiation damage by polyatomic cluster ion beams, micropatterning was performed on Si(100) and PMMA substrates. Line patterns with a width of 0.5, 1, and 3 μm, were prepared on Si(100) surfaces by ethanol cluster ion irradiation. Also, several periodic structures such as circles and squares with convex and concave types were formed at the microlevel using ethanol cluster ion irradiation. Furthermore, the micropatterning of PMMA substrates was demonstrated with water cluster ion beams. To demonstrate another application of materials processing, the wettability of Si(100) and Ti surfaces was investigated. The contact angle and FTIR measurements indicated that the surface modification was performed through the attachment of the radicals on the surface, which changed depending on the cluster ion species as well as the acceleration voltage.

ACKNOWLEDGMENTS

The authors are grateful to the Quantum Science and Engineering Center of Kyoto University for the Rutherford backscattering spectrometry (RBS) measurement. Also, this work was partially supported by Nanotechnology Support Project of the Ministry of Education, Culture, Sports, Science and Technology, Japan.

REFERENCES

1. H. Bernas and R.E. de Lamaestre: Ion beam-induced quantum dot synthesis in glass, in *Ion-Beam-Based Nanofabrication*, edited by D. Ila, J. Baglin, N. Kishimoto, and P.K. Chu (Mater. Res. Soc. Proc. **1020**, Warrendale, PA, 2007), p. 101.
2. W. Vandervorst and J.L. Everaert: E. Rosseel, M. Jurczak, T. Hoffman, P. Eyben, J. Mody, G. Zschatzsch, S. Koelling, M. Gilbert, T. Poon, J. Del Agua Borniquel, M. Foad, R. Duffy, and B.J. Pawlak: Conformal doping of FINFETs: A fabrication and metrology challenge, in *Proceedings of the 17th International Conference on Ion Implantation Technology IIT2008*, edited by E.G. Seebauer, S.B. Felch, A. Jain, and Y.V. Kondratenko (AIP Conf. Proc. **1066**, Melville, New York, 2008), p. 449.
3. L. Bardos and H. Barankova: Plasma processes at atmospheric and low pressures. *Vacuum* **83**, 522 (2009).
4. G. Brauer, B. Szyszka, M. Vergohl, and R. Bandorf: Magnetron sputtering—milestones of 30 years. *Vacuum* **83**, 1354 (2010).
5. J. Orloff, M. Utlaut, and L. Swanson: *High Resolution Focused Ion Beams: FIB and Its Applications* (Kluwer Academic/Plenum Publishers, New York, 2003).
6. D.J. Stokes, L. Roussel, O. Wilhelmi, L.A. Giannuzzi, and D.H.W. Hubert: Recent advances in FIB technology for nano-prototyping and nano-characterization, in *Ion-Beam-Based Nanofabrication*, edited by D. Ila, J. Baglin, N. Kishimoto, and P.K. Chu (Mater. Res. Soc. Proc. **1020**, Warrendale, PA, 2007), p. 15.
7. C.M. Lyneis, D. Leitner, D.S. Toda, G. Sabbi, S. Prestemon, S. Caspi, and P. Ferracin: Fourth generation electron cyclotron resonance ion sources. *Rev. Sci. Instrum.* **79**, 02A321 (2008).
8. J. Peters: New developments in multicusp H⁻ ion sources for high energy accelerators. *Rev. Sci. Instrum.* **79**, 02A515 (2008).
9. R.S. Hemsworth, A. Tanga and V. Antoni: Status of the ITER neutral beam injection system. *Rev. Sci. Instrum.* **79**, 02C109 (2008).
10. J. Ishikawa: Negative-ion source applications. *Rev. Sci. Instrum.* **79**, 02C506 (2008).
11. W. Jacob and J. Roth: Chemical Sputtering. In R. Behrisch, W. Eckstein(Eds.) *Sputtering by Particle Bombardment, Top. Appl. Phys. 110* (Springer, Berlin/Heidelberg/New York, 2007) p. 329.
12. Ph. Buffat and J-P. Borel: Size effect on the melting temperature of gold particles. *Phys. Rev. A* **13**, 2287 (1976).
13. M.D. Morse: Clusters of transition-metal atoms. *Chem. Rev.* **86**, 1049 (1986).
14. H. Hsieh and R.S. Averback: Molecular-dynamics investigation of cluster-beam deposition. *Phys. Rev. B* **42**, 5365 (1990).
15. R.S. Averback, M. Ghaly, and H. Zhu: Cluster solid interactions—A molecular-dynamics investigation. *Radiat. Eff. Defects Solids* **130-131**, 211 (1994).
16. Z. Insepov, I. Yamada, and M. Sosnowski: Sputtering and smoothing of metal surface with energetic gas cluster beams. *Mater. Chem. Phys.* **54**, 234 (1998).
17. M. Moseler, O. Rattunde, J. Nordiek, and H. Haberland: On the origin of surface smoothing by energetic cluster impact: Molecular dynamics simulation and mesoscopic modeling. *Nucl. Instrum. Methods B* **164-165**, 522 (2000).
18. H. Yasumatsu and T. Kondow: Reactive scattering of clusters and cluster ions from solid surfaces. *Rep. Prog. Phys.* **66**, 1783 (2003).
19. G.H. Takaoka, K. Nakayama, T. Okada, and M. Kawashita: Size analysis of ethanol cluster ions and their sputtering effects on solid surfaces, in *Proceedings of the 16th International Conference on Ion Implantation Technology*, edited by K.J. Kirkby, R. Gwilliam, A. Smith, and D. Chivers (AIP Conf. Proc., 2006), p. 321.
20. G.H. Takaoka, M. Kawashita, and T. Okada: Irradiation effects of methanol cluster ion beams on solid surfaces, in *Ion-Beam-Based Nanofabrication*, edited by D. Ila, J. Baglin, N. Kishimoto, and P.K. Chu (Mater. Res. Soc. Proc. **1020**, Warrendale, PA, 2007), p. 159.
21. G.H. Takaoka, M. Kawashita, and T. Okada: Physical and chemical sputtering of solid surfaces irradiated by ethanol cluster ion beams. *Rev. Sci. Instrum.* **79**, 02C503 (2008).
22. H. Ryuto, K. Tada, and G.H. Takaoka: Irradiation effects on solid surfaces by water cluster ion beams. *Vacuum* **84**, 501 (2010).
23. G.H. Takaoka, H. Noguchi, K. Nakayama, Y. Hironaka, and M. Kawashita: Fundamental characteristics of liquid cluster ion source for surface modification. *Nucl. Instrum. Methods B* **237**, 402 (2005).
24. H. Haberland: *Clusters of Atoms and Molecules* (Springer-Verlag, Berlin, 1994).
25. J. Merikanto, H. Vehkamäki, and E. Zapadinsky: Monte Carlo simulations of critical cluster sizes and nucleation rates of water. *Chem. Phys.* **121**, 914 (2004).
26. P. Wegener: *Nonequilibrium Flows* (Marcel Dekker, New York, 1969).
27. R.C. Weast and M.J. Astle (Eds.): *CRC Handbook of Physics and Chemistry*, 63rd ed. (CRC Press, Boca Raton, FL, 1982).
28. R.C. Tolman: The effect of droplet size on surface tension. *Chem. Phys.* **17**, 333 (1949).
29. O.F. Hagena and W.J. Obert: Cluster formation in expanding supersonic jets – effect of pressure, temperature, nozzle size, and test gas. *Chem. Phys.* **56**, 1793 (1972).
30. O.F. Hagena: Scaling laws for condensation in nozzle flows. *Phys. Fluids* **17**, 894 (1974).
31. O.F. Hagena: Cluster ion sources. *Rev. Sci. Instrum.* **63**, 2374 (1992).
32. P. Borowski, J. Jaroniec, T. Janowski, and K. Wolinski: Quantum cluster equilibrium theory treatment of hydrogen-bonded liquids: Water, methanol and ethanol. *Mol. Phys.* **101**, 1413 (2003).
33. Z. Insepov, M. Sosnowski, and I. Yamada: Molecular-dynamics simulation of metal surface sputtering by energetic rare-gas cluster impact. *Trans. Mater. Res. Soc. Jpn.* **17**, 111 (1994).
34. W.D. Kingery, H.K. Bowen, and D.R. Uhlmann: *Introduction to Ceramics* (John Wiley & Sons Inc., New York, 1976) Chap. 9.
35. Z. Insepov, M. Sosnowski, G.H. Takaoka, and I. Yamada: Molecular dynamics simulation of the effects of energetic cluster ion impact on solid surface, in *Materials Synthesis and Processing Using Ion Beams*, edited by R.J. Culbertson, O.W. Holland, K.S. Jones, and K. Maex (Mater. Res. Soc. Proc. **316**, 1994), p. 999.
36. Z. Insepov and I. Yamada: Molecular-dynamics simulation of surface sputtering by energetic rare-gas cluster impact. *Surf. Rev. Lett.* **3**, 1023 (1996).
37. H. Ryuto, R. Ozaki, H. Mukai, and G.H. Takaoka: Interaction of ethanol cluster ion beam with silicon surface. *Vacuum* **84**, 1419 (2010).
38. L. Maissel: in *Handbook of Thin Film Technology*, edited by L.I. Maissel and R. Glang (McGraw-Hill, New York, 1970) Chap. 4.
39. K.L. Chopra: Thin Film Deposition Technology. *Thin Film Phenomena* (McGraw-Hill, New York, 1979) Chap. 2.
40. F. Frost, R. Fechner, B. Ziberi, D. Flamm, and A. Schindler: Large area smoothing of optical surfaces by low-energy ion beams. *Thin Solid Films* **459**, 100 (2004).
41. W. Eckstein: Sputtering Yields. In R. Behrisch and W. Eckstein (Eds.) *Sputtering by Particle Bombardment, Top. Appl. Phys. 110* (Springer, Berlin/Heidelberg/New York, 2007) p. 33.
42. T. Seki, T. Kaneko, D. Takeuchi, T. Aoki, J. Matsuo, Z. Insepov, and I. Yamada: STM observation of HOPG surfaces irradiated with Ar cluster ions. *Nucl. Instrum. Methods B* **121**, 498 (1997).
43. S.T. Picraux and L.E. Pope: Tailored surface modification by ion implantation and laser treatment. *Science* **226**, 615 (1984).
44. R. Langer: Perspectives: Drug delivery-drugs on target. *Science* **293**, 58 (2001).

45. H. Lee, S.M. Dellatore, W.M. Miller, and P.B. Messersmith: Mussel-inspired surface chemistry for multifunctional coatings. *Science* **318**, 426 (2007).
46. M. Carbone, M.N. Piancastelli, J.J. Paggel, C. Weindel, and K. Horn: A high-resolution photoemission study of ethanol adsorption on Si(111)-(7x7). *Surf. Sci.* **412-413**, 441 (1998).
47. M.P. Casaletto, R. Zaroni, M. Carbone, M.N. Piancastelli, L. Aballe, K. Weiss, and K. Horn: High-resolution photoemission study of ethanol on Si(100)2x1. *Surf. Sci.* **447**, 237 (2000).
48. P.L. Silvestrelli: Adsorption of ethanol on Si(100) from first-principles calculations. *Surf. Sci.* **552**, 17 (2004).
49. G.G. Roberts (Ed.): *Langmuir-Blodgett Films* (Plenum, New York, 1990) Chap.7.
50. S.R. Whaley, D.S. English, E.L. Hu, P.F. Barbara, and A.M. Belcher: Selection of peptides with semiconductor binding specificity for directed nanocrystal assembly. *Nature* **405**, 665 (2000).
51. J.C. Love, L.A. Estroff, J.K. Kriebel, R.G. Nuzzo, and G.M. Whitesides: Self-assembled monolayers of thiolates as a form of nanotechnology. *Chem. Rev.* **105**, 1103 (2005).